JOURNAL OF NEUROTRAUMA 34:3336–3350 (December 15, 2017)
© Mary Ann Liebert, Inc.
DOI: 10.1089/neu.2017.5034

Changes in Pressure, Hemodynamics, and Metabolism within the Spinal Cord during the First 7 Days after Injury Using a Porcine Model

Femke Streijger,[1] Kitty So,[1] Neda Manouchehri,[1] Seth Tigchelaar,[1] Jae H.T. Lee,[1] Elena B. Okon,[1] Katelyn Shortt,[1] So-Eun Kim,[1] Kurt McInnes,[1,2] Peter Cripton,[1,2] and Brian K. Kwon[1,3]

Downloaded by UNIVERSITE DE SHERBROOKE from www.liebertpub.com at 03/09/18. For personal use only.

Abstract

Traumatic spinal cord injury (SCI) triggers many perturbations within the injured cord, such as decreased perfusion, reduced tissue oxygenation, increased hydrostatic pressure, and disrupted bioenergetics. While much attention is directed to neuroprotective interventions that might alleviate these early pathophysiologic responses to traumatic injury, the temporo-spatial characteristics of these responses within the injured cord are not well documented. In this study, we utilized our Yucatan mini-pig model of traumatic SCI to characterize intraparenchymal hemodynamic and metabolic changes within the spinal cord for 1 week post-injury. Animals were subjected to a contusion/compression SCI at T10. Prior to injury, probes for microdialysis and the measurement of spinal cord blood flow (SCBF), oxygenation (in partial pressure of oxygen; $PaPO_2$), and hydrostatic pressure were inserted into the spinal cord 0.2 and 2.2 cm from the injury site. Measurements occurred under anesthesia for 4 h post-injury, after which the animals were recovered and measurements continued for 7 days. Close to the lesion (0.2 cm), SCBF levels decreased immediately after SCI, followed by an increase in the subsequent days. Similarly, $PaPO_2$ plummeted, where levels remained diminished for up to 7 days post-injury. Lactate/pyruvate (L/P) ratio increased within minutes. Further away from the injury site (2.2 cm), L/P ratio also gradually increased. Hydrostatic pressure remained consistently elevated for days and negatively correlated with changes in SCBF. An imbalance between SCBF and tissue metabolism also was observed, resulting in metabolic stress and insufficient oxygen levels. Taken together, traumatic SCI resulted in an expanding area of ischemia/hypoxia, with ongoing physiological perturbations sustained out to 7 days post-injury. This suggests that our clinical practice of hemodynamically supporting patients out to 7 days post-injury may fail to address persistent ischemia within the injured cord. A detailed understanding of these pathophysiological mechanisms after SCI is essential to promote best practices for acute SCI patients.

Keywords: blood flow; L/P ratio; microdialysis; oxygenation; porcine model; pressure; spinal cord injury

Introduction

Acute trauma to the spinal cord can result in devastating neurologic impairment for which there currently remains few treatment options that can be offered to improve neurologic function. While the primary damage to the spinal cord occurs at the time of mechanical impact (e.g., from a motor vehicle accident, fall from height), early treatment approaches for the acutely injured patient aim to mitigate the secondary pathophysiologic processes that are triggered within the injured cord. These include vascular disruption, intraparenchymal hemorrhage, vasospasm, impaired autoregulation, and vasogenic edema as a consequence of blood–spinal cord barrier breakdown.[1] These combined responses can lead to impaired spinal cord perfusion with resultant ischemia, hypoxia, and energy dysfunction, of which all can negatively impact spared neural tissue at and around the injury site.[2] Therefore, current clinical practice guidelines encourage aggressive hemodynamic resuscitation and elevation of mean arterial blood pressure (MAP) to 85–90 mm Hg for the first 7 days post-injury.[3–6] Recent clinical evidence suggests that the elevation of MAP and the avoidance of hypotension are indeed beneficial for neurologic recovery in acute spinal cord injury (SCI) patients.[7]

Given that the hemodynamic management of acute SCI appears to represent an opportunity to influence neurologic outcome, an understanding of the post-traumatic alterations in spinal cord perfusion and the downstream metabolic consequences is essential. Our current understanding of the spatial and temporal dynamics of the changes in perfusion within the acutely injured spinal cord is

[1]International Collaboration on Repair Discoveries (ICORD), [2]Departments of Mechanical Engineering and Orthopedics, [3]Vancouver Spine Surgery Institute, Department of Orthopedics, University of British Columbia, Vancouver, British Columbia, Canada.

Downloaded by UNIVERSITE DE SHERBROOKE from www.liebertpub.com at 03/09/18. For personal use only.

limited. There is a considerable body of pre-clinical literature that has provided fundamental insights into the changes in spinal cord blood flow (SCBF) after traumatic injury.[2,8–12] However, most of these studies employ rodent models and induce injury to the spinal cord with extradural clip compression for 1 min up to 40 min, at most.[10–13] Extrapolating these data to the human condition is therefore challenging where the spinal cord is much larger, compression can be sustained for many hours, and the typical period of hemodynamic support extends for a full week post-injury.

Further, while much of the pre-clinical literature has focused on alterations in SCBF, it is ultimately desirable to understand the subsequent downstream metabolic consequences of these changes within the areas of potentially vulnerable spinal cord tissue. As the balance between SCBF and metabolic demand for oxygen influences whether the tissue is hypoxic or not, monitoring SCBF alone may not provide a complete assessment of the metabolic insult within the injury penumbra. As such, simultaneously measuring spinal cord oxygenation and downstream metabolic changes in addition to SCBF would allow for a more comprehensive assessment of the tissue hemodynamics. To our knowledge, such a combined approach of directly measuring SCBF, oxygenation, pressure, and metabolites from the spinal cord parenchyma continuously for days after injury has not been previously reported.

In previous work, we used intraparenchymal spinal cord microdialysis in our porcine model of SCI to measure the extent to which energy-related substrates such as lactate, pyruvate, and glucose were affected for the first 4 h post-injury.[14] Our data reveal significant and prolonged tissue ischemia and hypoxia at the injury site after contusion-compression SCI, marked by a dramatic increase in lactate/pyruvate (L/P) ratio (> 700% of pre-injury levels), with a concurrent fall in glucose levels (< 50%) within the first 20 min post-injury.[14] It also was evident that the observed metabolic changes had not plateaued or normalized at the conclusion of the experiment 4 h post-injury. Therefore, in the present study, we extend these observations by continuing these intraparenchymal microdialysis measurements for a full 7 days post-injury, while also measuring SCBF, oxygenation (in partial pressure of oxygenation; $PaPO_2$), and hydrostatic pressure to investigate the relationship between these important physiologic variables.

Methods

All animal protocols and procedures employed in this study were approved by the Animal Care Committee of the University of British Columbia and were compliant with the policies of the Canadian Council of Animal Care.

Animals and housing

Female miniature Yucatan pigs (Sinclair Bio-resources, Columbia, MO) were transported to our animal facility 5 weeks before surgery. Upon arrival, the animals were housed in groups of four in an indoor pen bedded with sawdust and toys (chains, balls) with access to an adjoining outdoor pen. Animals were given water *ad libitum* and fed 1.5% of their body weight twice a day (Mazuri Mini-Pig Youth; PMI Nutrition International, Brentwood MO). Each pig was individually handled for at least 15 min daily to improve the comfort level with human contact.

Porcine model of SCI

Prior to the day of surgery, animals were fasted for 12 h. Tracheal intubation and mechanical ventilation was performed as described previously.[15,16] Anesthesia was maintained with a combination of isoflurane (0.5% in 100% O_2) and propofol (8–20 mg/kg/h; Baxter, Allison, Ontario). All animals received ketoprofen (3 mg/kg) via intravenous administration and fentanyl (15–30 μg/kg/h; Sandoz Canada, Boucherville, Quebec) delivered via continuous rate infusion. After a surgical plane of anesthesia was reached, a skin incision was made along the dorsal midline of the thoracic region of each animal. Using electro-cautery (Surgitron Dual Frequency RF/120 Device; Ellman International, Oceanside, NY), the semispinalis, multifidus, and longissimus lumborum muscles were separated from the dorsal spinous processes and laminae. A T9 to T13 laminectomy was performed and widened to expose the dura and spinal cord with sufficient clearance for sensor insertion and weight-drop injury.

The SCI was delivered by a weight drop impactor device, which was securely fixed to the spine using an articulating arm (660; Starrett, Athol, MA) mounted via bilaterally inserted T6 and T8 pedicle screws. This arm enabled the guide-rail to be precisely positioned and aligned, allowing for the impactor to fall straight vertically onto the exposed dura and cord at T10. The tip of the impactor (diameter, 0.953 cm) was outfitted with a load cell (LLB215; Futek Advanced Sensor Technology, Irvine, CA) to record the force at impact. The guide rail was equipped with a Balluff Micropulse linear position sensor (BTL6-G500-M0102-PF-S115; Balluff Canada Inc., Mississauga, Ontario) to record the impactor position from 10 cm above the impact (for calculation of impact velocity and cord displacement). A custom controller was used to operate the device and filter the force and position data was collected with the simultaneous USB DAQ module (DT9816-S; Data Translation Inc., Marlboro, MA). A LabVIEW (National Instruments, Austin, TX) program enabled remote operation of the device and real-time data collection feedback.

Immediately after the weight-drop contusion injury (weight, 50 g; height, 50 cm), sustained compression was maintained on the contused spinal cord for 1 h by placing an additional 100 g weight onto the impactor (150 g total). The weight of the impactor (50 g), height of the weight drop (50 cm), and duration of compression with the additional 100 g weight (1 h) were chosen so as to replicate the injury parameters of our previous study in which we performed similar intraparenchymal microdialysis measurements for 4 h post-SCI.[14] Our current experiment was intended to extend the findings of this previous study.

Insertion of the intraparenchymal blood flow/O_2, pressure, and microdialysis probes

To consistently insert the monitoring probes into a desired location within the spinal cord and to maintain their position for the duration of the experiment, a custom-made sensor holder was created (Fig. 1). The sensor holder was attached rigidly to the spine via bilateral T9, T11, T12, and T14 pedicle screws (Select Multi Axial Screw; Medtronic, Minneapolis, MN) and 3.5 mm titanium rods (Medtronic). The location of the sensor holder was locked in place by sliding the device over the rod and adjusting the height of the pedicle screws. Additional transverse connecting bridges were fixed between two polyaxial pedicle screws to produce a stable, rigid construct. Six custom-made introducers with a lumen wide enough to fit one sensor/probe were inserted through precision-drilled holes in the sensor-holder (holes were drilled at a 45-degree angle relative to the holder; Fig. 1), entering the dura at approximately 1.2 and 3.2 cm from the center of the intended impact. Subsequently, the sensors were guided through the introducers and advanced another 0.2 cm, placing the sensors in the ventral aspects of the white matter (Fig. 2). The distance between adjacent tip locations was 0.5–1.0 mm. The final location of the tip of the sensors were situated approximately 0.2 cm and 2.2 cm away from the edge of intended impact location. Ultrasound imaging (L14-5/38, 38 mm linear array probe, Ultrasonix RP; BK Ultrasound, Richmond, British Columbia) was utilized to verify accurate positioning of sensors and probes into the cord (Fig. 2). To prevent

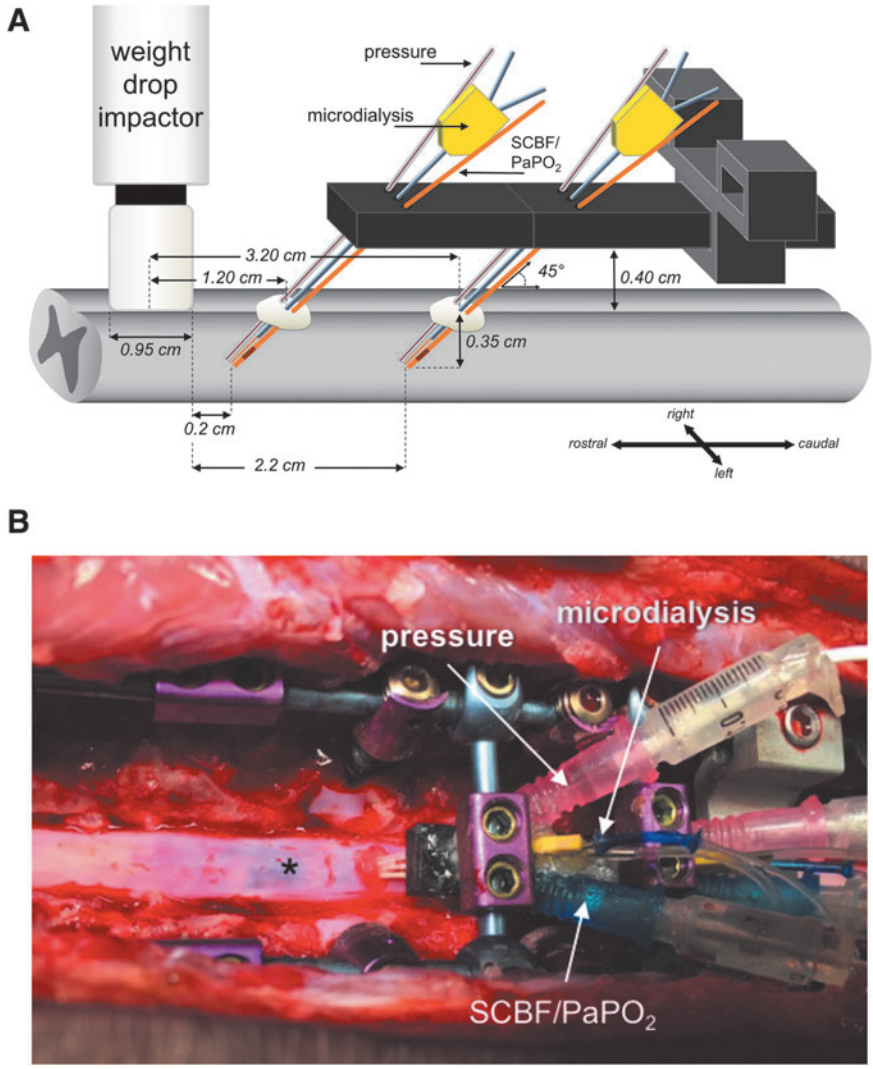

FIG. 1. Intraparenchymal monitoring set-up for inserting and securing SCBF/$PaPO_2$, pressure, and microdialysis probes within the spinal cord. This figure illustrates the fixation device, which is secured rigidly via the pedicle screw/rod construct to the spinal column. The device has three independently drilled channels through which the SCBF/$PaPO_2$ (left), pressure (right), and microdialysis (middle) probes are inserted. The probes penetrate the dura 1.2 cm and 3.2 cm caudal from the anticipated epicenter of the contusion impact and are advanced approximately 14 mm at a 45° angle. As the impactor is 0.95 cm in diameter, the final location of the sensor tips are approximately 0.2 cm and 2.2 cm away from the edge of the impactor. *Spinal cord injury hemorrhage. SCBF, spinal cord blood flow; $PaPO_2$, partial pressure of oxygen. Color image is available online at www.liebertpub.com/neu

Downloaded by UNIVERSITE DE SHERBROOKE from www.liebertpub.com at 03/09/18. For personal use only.

cerebrospinal fluid (CSF) leakage, cyanoacrylate glue was applied to the dural surface where the catheters entered. After sensor insertion, a 2-h period was given to allow ''stabilization'' before recording the ''baseline'' samples for a period of 60 min prior to SCI.

Measure of intraparenchymal blood flow and $PaPO_2$

For measurement of blood flow and oxygen, we utilized a single multi-parameter probe that at the tip contains both a sensor for measuring flow and another for measuring $PaPO_2$. This probe with a tip diameter of 450 μm (NX-BF/OF/E; Oxford Optronix, Oxford, UK) was connected to the OxyLab/OxyFlo combined channel monitor (OxyLab: Oxford Optronix) with LabChart Pro software for interpretation (ADInstruments, Colorado Springs, Colorado,). $PaPO_2$ was measured by a fluorescence quenching technique, which monitors the mean time between photon absorption and emission of the oxygen-sensitive fluorescent ruthenium lumiphor dye after being excited by a short pulse of light (luminescence lifetime). In the presence of oxygen, the fluorescence lifetime is quenched proportionally to the oxygen concentration. The OxyLab system measures the reduced lifetime of luminescence of the reflected signal and displays a value for $PaPO_2$ in mm Hg. Since the luminescence-based oxygen sensing technique is sensitive to temperature changes, a thermocouple transducer is incorporated into the sensor to correct for temperature variations within its operating range of 30–44°C. Blood flow is determined via laser-Doppler flowmetry (LDF) where light from the probe tip is projected into the tissue, scattered, then reabsorbed by a sensor. Only the laser light backscattered from moving cells undergoes a Doppler shift, which creates Doppler frequencies at the detectors to produce a voltage output that can be interpreted as blood flow by the OxyFlo monitor (in arbitrary perfusion units, BPU). The numeric calculation of LDF is dependent on the relative concentration of local red blood cells in the tissue and the velocity.

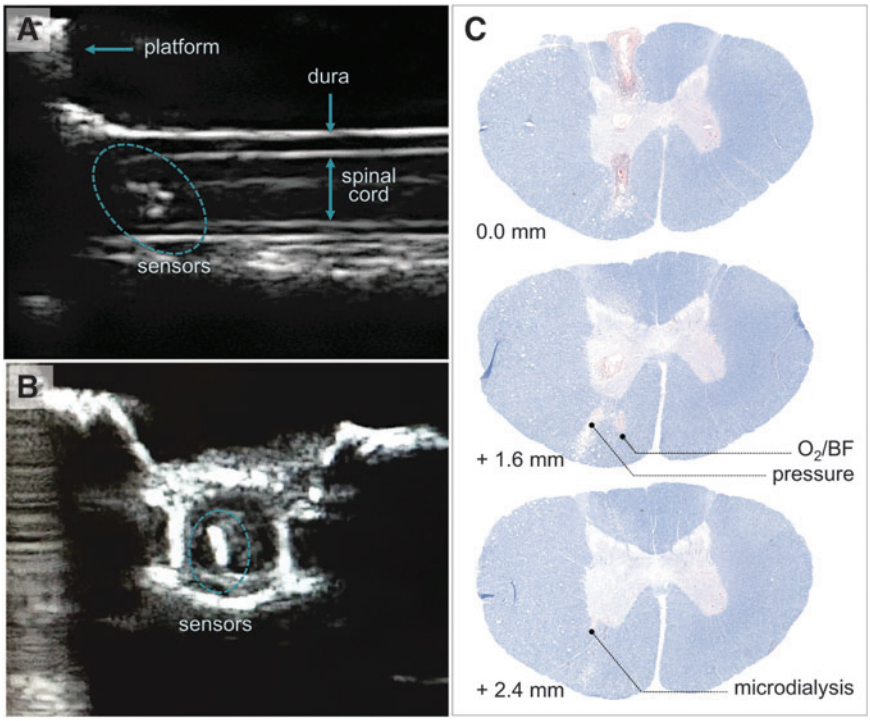

FIG. 2. Evaluation of intraparenchymal probe position with ultrasound and histologic methods. Representative ultrasound images in both **(A)** midsagittal and **(B)** axial planes showing the location of the probes within the parenchyma of the spinal cord at the time of surgery. Each probe was advanced through the spinal cord at a 45° angle. The dorso-ventral diameter of the porcine spinal cord was ~5.5 mm at this level (T10); the diameter of the subarachnoid space was ~9 mm. **(C)** Eriochrome Cyanine R–stained spinal cord section from 7-day post-injury revealed that the final locations of the probe tips were in the ventral aspects of the white matter. In this example, the tips of the SCBF/$PaPO_2$ and pressure probes were situated +1.6 mm from the initial point of entry (0.0 mm); the tip of the microdialysis probe was situated +2.4 mm rostral from the initial point of entry. In all animals studied, the anterior-posterior distance between adjacent tip locations ranged between 0.5 and 1.0 mm. SCBF, spinal cord blood flow; $PaPO_2$, partial pressure of oxygen. Color image is available online at www.liebertpub.com/neu

Intraparenchymal pressure measurement

Spinal cord pressure was characterized using custom-manufactured fiber optic pressure transducers (FOP-LS-NS-1006A; FISO Technologies Inc., Harvard Apparatus, Quebec) with a sensor tip diameter of 333 μm. This technology has been used in previous studies to measure CSF pressure *in vivo* in spinal cord injured pigs,[17] intracranial pressure during blast and shock waves in rats[18,19] and pigs,[20] pressure in the nucleus of the intervertebral discs,[21] and was recently evaluated for monitoring pressure in spinal cord tissue.[22]

The sensor tip is comprised of two parallel reflecting mirrors on either side of an optical cavity. The first mirror is semi-reflective and the second is a flexible membrane. As pressure is applied, the membrane deflects, reducing the cavity length. The reduced cavity lengths cause phase shifts in the reflected light, which are distinguished by a detector. Transducers are calibrated in such way that each cavity length corresponds to a specific pressure value, with the transducers being capable of measuring pressure changes of ±300 mm Hg, with a resolution of ±0.3 mm Hg. Transducers were connected to a chassis-mounted signal conditioner module (EVO-SD-5/FPI-LS-10; FISO Technologies Inc., Harvard Apparatus) with internal atmospheric pressure compensation, which is particularly valuable for long-term animal studies. The data was acquired digitally through the Evolution software (FISO Technologies Inc., Harvard Apparatus) at a frequency of 1 Hz.

Microdialysis

Microdialysis probes (CMA11, CMA Microdialysis; Harvard Apparatus) with an outer diameter of 380 μm, 2 mm membrane length, and a 6-kDa cutoff were used to sample the extracellular fluid for energy related metabolites. Probes were continuously perfused with artificial CSF (Perfusion Fluid CNS, CMA Microdialysis; Harvard Apparatus) using a subcutaneous implantable micro-pump at a flow rate of 0.5 μl/min (SMP-200, IPrecio, Alzet Osmotic Pumps; Durect Corporation, Cupertino, CA). Dialysates were collected every 15 min in micro tubes, capped, and frozen on dry ice from the beginning of the baseline period to 6 h post-injury, and then every 12 h, providing a sample volume of 7.5 μL sufficient for the exploration of five metabolites (lactate, pyruvate, glucose, glutamate, and glycerol). Samples were analyzed within a week of collection using the ISCUSflex Microdialysis Analyzer (M Dialysis, Stockholm, Sweden). Measured sample concentrations below the manufacturer's indicated linear range of the assays were replaced with the minimum linear range value.

Post-operative recovery and continuous monitoring

Anesthesia and mechanical ventilation with 100% oxygen were stopped at 4 h after SCI and the animal was extubated on room air. Between animals there was a 5–10-min variability in anesthesia duration. Subsequently within 2 h (i.e., between 4–6 h post-injury), animals were returned to their respective recovery enclosures for 7 days.

Post-surgical pain control was managed with fentanyl via constant rate infusion (2–12 mcg/kg/h intravenously) for the first 7 days after surgery. Animals were given tramadol (1–2 mg/kg; orally), and received enrofloxacin (5mg/kg; subcutaneously) daily for at least 3 days as an antibiotic, and ketoprofen (3 mg/kg;

Downloaded by UNIVERSITE DE SHERBROOKE from www.liebertpub.com at 03/09/18. For personal use only.

intramuscularly) once a day for 3 days as an anti-inflammatory agent. Urinary catheters remained in place until the animals were able to reflexively empty their bladders, usually within 7–10 days. If fecal production was low and the animals appeared to be experiencing stasis in the gastrointestinal tract, a constant rate infusion of metaclopramide (5 mg/mL at 0.01–0.02 mg/kg/h) and lactulose (5 mL) was administered. Sucralfate (5 mL) was given if an animal experienced anorexia and/or bloating.

Sensor cables were kept away from the animal's reach using a custom-designed counter-balanced lever system, and the microdialysis collection lines and tubes were securely placed into a harness worn by the animal (Fig. 3). This set-up allowed for continuous recording and sampling over 7 days without the need to disconnect and reconnect the monitoring wires.

Eriochrome Cyanine R staining

Spinal cord segments were fixed in 4% PFA and cryoprotected using graded concentrations of sucrose (6, 12, 24% sucrose in 0.1 M Phosphate Buffer each for 48 h). Tissue was then transversely cut in 20-μm sections and stained with Eriochrome Cyanine R as described previously.[15,16,23] The distribution of spared white and grey matter was mapped using digital color images taken at 800-μm intervals throughout the lesion site (Zeiss AxioImager M2 microscope) and analyzed using Zen Imaging Software (Carl Zeiss Canada Ltd., Toronto, Ontario). The extent of spared white matter and gray matter were calculated as the percentage of total area of the spinal cord (i.e., area within the tracing of spinal cord perimeter), with lesion epicenter located centrally.

Data analysis

SCBF and $PaPO_2$ were recorded continuously at a sampling rate of 10 and 1 Hz respectively during baseline recording and for 3 h after SCI. Thereafter, the sampling rate for $PaPO_2$ was reduced to 1/60 Hz, as the sensor carries only a limited supply of the ruthenium lumiphor. To mitigate movement artifacts in the oxygenation and blood flow data, a post-processing filter was applied (smoothing type, median filter; window width, 601 samples/1 min of sampling). For SCBF, $PaPO_2$, and pressure data, values were averaged over 15-min intervals for the first 24 h and into 60-min bins after the first 24 h. Microdialysis samples were collected every 15 min from the beginning of the baseline period to 6 h post-injury. After 6 h, dialysates were taken in duplicate at 15-min intervals every 12 h. These duplicate values were averaged for each time-point. The delay from microdialysis catheter tip to collecting vial was 12 mins, and this was accounted for when analyzing the results. The lactate to pyruvate (L/P) ratio was calculated from the measured values of lactate and pyruvate concentrations. To account for absolute differences in the baseline recordings, all values were expressed as a percentage change from baseline (% from baseline) as a function of time (min). Results are expressed as mean values (± standard error of the mean), with correlations between parameters determined using Spearman correlation coefficients with Bonferroni correction (GraphPad Prism 6).

Results

Injury parameters

Eight animals received a contusion SCI by dropping a 50 g weight from a 50 cm height at the T10 level of the spinal cord followed by 1 h of compression (150 g total weight). The maximum impact force applied to the exposed spinal cord measured at the tip of the impactor was on average 5443 ± 438 kdynes (Table 1). The impactor tip traveled 6.36 ± 0.30 mm from initial contact with the exposed dura with a velocity of 2736 ± 102 mm/sec at impact. Such contusion-compression injury resulted in a compete loss of gray and white matter at center of the impact (T10), with loss of white and gray matter at distances up to 10–13 mm from the epicenter in both rostral and caudal directions (Fig. 4).

Post-injury changes in intraparenchymal pressure, blood flow, $PaPO_2$, and pressure

At the 0.2-cm position (i.e., the more proximal of the two sensor insertion points), intraparenchymal spinal cord pressure, which started at 10.4 ± 1.0 mm Hg drastically increased ~370% (an absolute difference of about 35 mm Hg) of baseline values and remained elevated while residual compression remained on the cord (Fig. 5A). Following decompression, the pressure immediately dropped back to slightly above baseline values. After this transient fall, the pressure gradually increased once again to reach a maximum of ~220% of baseline (an absolute difference of about 14 mm Hg) at 4.5 h post-SCI. After 15 h, a slight decrease in pressure was observed, although values remained above baseline levels for the 7 days of observation (~150%; an absolute difference of about 5 mm Hg).

SCBF and $PaPO_2$ levels fell rapidly below baseline levels following SCI and while the spinal cord remained compressed (Fig. 5B, 5C). Following decompression, both SCBF and $PaPO_2$

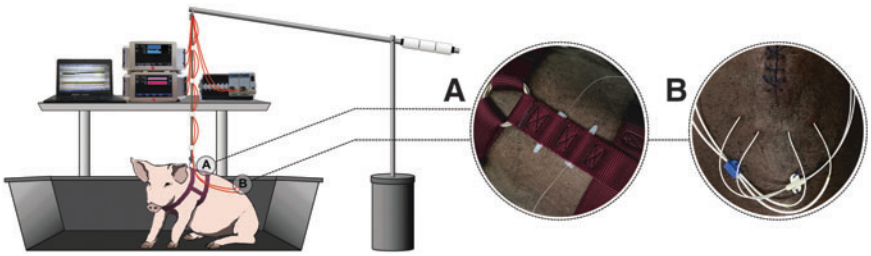

FIG. 3. Post-operative set-up for continuous microdialysis sampling and monitoring of SCBF/$PaPO_2$ and pressure for a total of 7-days after SCI. SCBF/$PaPO_2$, pressure, and microdialysis probes were inserted into the spinal cord 0.2 and 2.2 cm away from the edge of the initial impact **(A)** To achieve microdialysis samples over 7 days, we used a miniature infusion pump (iPRECIO) for dialysate inflow that was implanted and left within the animal. The outflow tubing for each microdialysis catheter was tunneled percutaneously out to a collection vial (*) and secured via a harness to the upper thoracic region of the animal. **(B)** The SCBF/$PaPO_2$ and pressure probes were also tunneled percutaneously and attached to a lead, connecting the harness to the counter-balance lever system that was positioned above the center of the pen. The lever system with counterweights ensured the sensor wires were held out of the animals' reach at all times so that they could not be chewed on or otherwise disrupted, yet still allowed free movement of the animals within the enclosure. SCBF, spinal cord blood flow; SCI, spinal cord injury; $PaPO_2$: partial pressure of oxygen. Color image is available online at www.liebertpub.com/neu

Downloaded by UNIVERSITE DE SHERBROOKE from www.liebertpub.com at 03/09/18. For personal use only.

Table 1. Measures of Age, Body Weight, and Injury

Age (months) [Average ± SEM]	*Body weight (kg) [Average ± SEM]*	*Max force (kdynes) [Average ± SEM]*	*Displacement (mm) [Average ± SEM]*	*Impact velocity (mm/sec) [Average ± SEM]*
4.57	23.0	6004	6.75	2935
4.77	23.0	5310	6.11	2835
5.23	24.0	5128	5.63	2542
4.40	24.5	5048	7.33	2911
3.83	22.5	5227	6.93	2826
4.00	23.5	8075	6.92	2917
4.00	23.5	3712	4.73	2091
4.47	20.0	5039	6.47	2838
[4.4 ± 0.2]	**[23.0 ± 0.5]**	**[5443 ± 438]**	**[6.36 ± 0.30]**	**[2736 ± 102]**

SEM, standard error of the mean.

Downloaded by UNIVERSITE DE SHERBROOKE from www.liebertpub.com at 03/09/18. For personal use only.

recovered slightly in the first few minutes, but remained below baseline levels for the next 3 h (~25% of baseline for $PaPO_2$ and ~60% of baseline for SCBF). Thereafter, SCBF showed a modest but continuous increase with time to about 150% of the baseline value. At around 4–6 h post-injury, the anesthesia and mechanical ventilation with 100% oxygen were stopped, and the animal was extubated on room air. This coincided with increased spinal cord perfusion and a dramatic drop in $PaPO_2$ levels to ~8% of baseline. Starting at around 24 h post-injury, the SCBF steadily increased to about 200% of baseline at the 7-day post-injury time-point. Despite this increase in SCBF, the $PaPO_2$ levels stayed fairly constant and remained at 8–10% of baseline values until the end of the study.

At the 2.2-cm position (i.e., the more distal of the two sensor positions), only modest changes in SCBF, $PaPO_2$, and pressure were observed following traumatic contusion, during sustained compression, and after decompression (Fig. 6). Notably, $PaPO_2$ dropped drastically after anesthesia and mechanical ventilation were discontinued (~4 h post-SCI). Thereafter, $PaPO_2$ continued to decrease for up to 48 h post-injury, after which it leveled off and remained low (Fig. 6). There was also a slight increase in intraparenchymal pressure at 4 h post-injury and remained elevated (albeit very slightly) for the duration of the experiment.

Post-injury changes in microdialysis markers

Time-dependent post-injury changes in microdialysis markers of excitotoxicity and membrane damage (glutamate and glycerol) and energy metabolism (glucose, lactate, and pyruvate) are summarized in Figure 7 and Figure 8, respectively.

At the 0.2-cm position, a sharp increase in glutamate levels was detected, reaching a peak increase of ~6000% within 15 min after contusion (Fig.7A; solid circles) and rapidly declined thereafter. This decreasing trend continued for another 2–3 h after decompression when glutamate reached high steady-state levels of

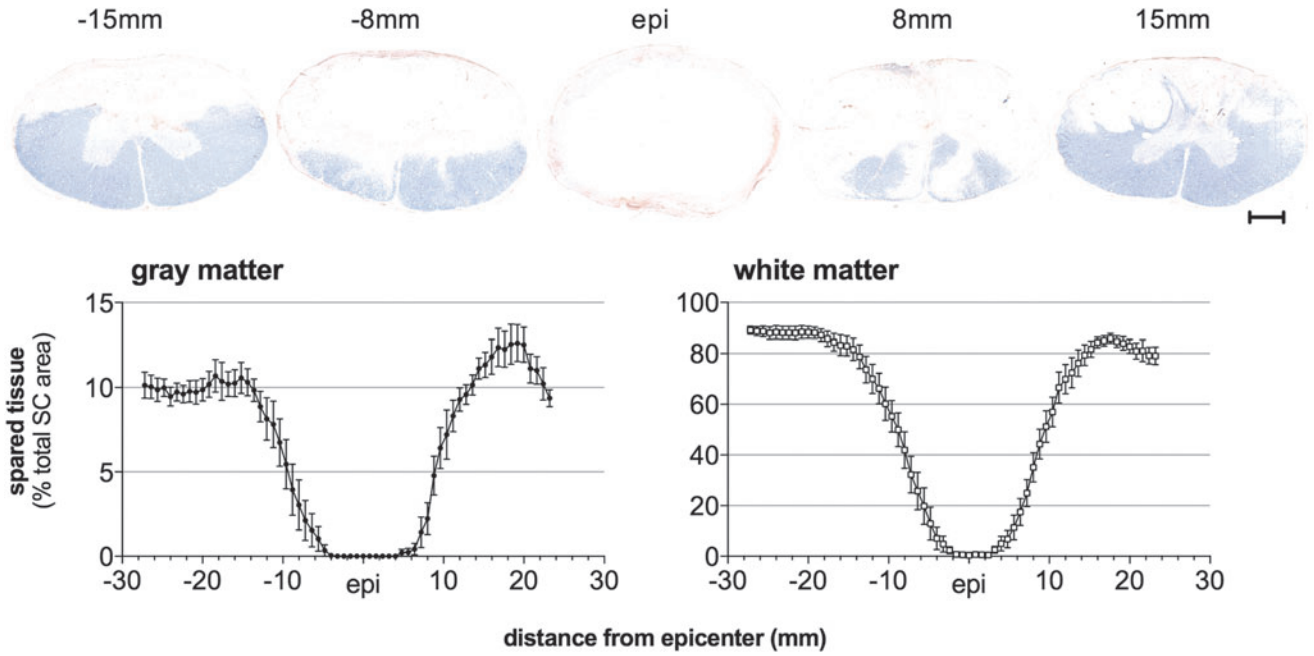

FIG. 4. Spared tissue analyses of Eriochrome Cyanine R–stained spinal cords. Spared gray and white matter determined by area measurements taken from axial sections of porcine spinal cord tissue 800 μm apart. Our T10 50-g/50-cm contusion injury model followed by 1 h of compression resulted in significant tissue damage extending 10–13 mm away from the lesion epicenter (''epi'') in both rostral-caudal directions. The values are means ± standard error of the mean. Scale bar: 1 mm. Color image is available online at www.liebertpub.com/neu

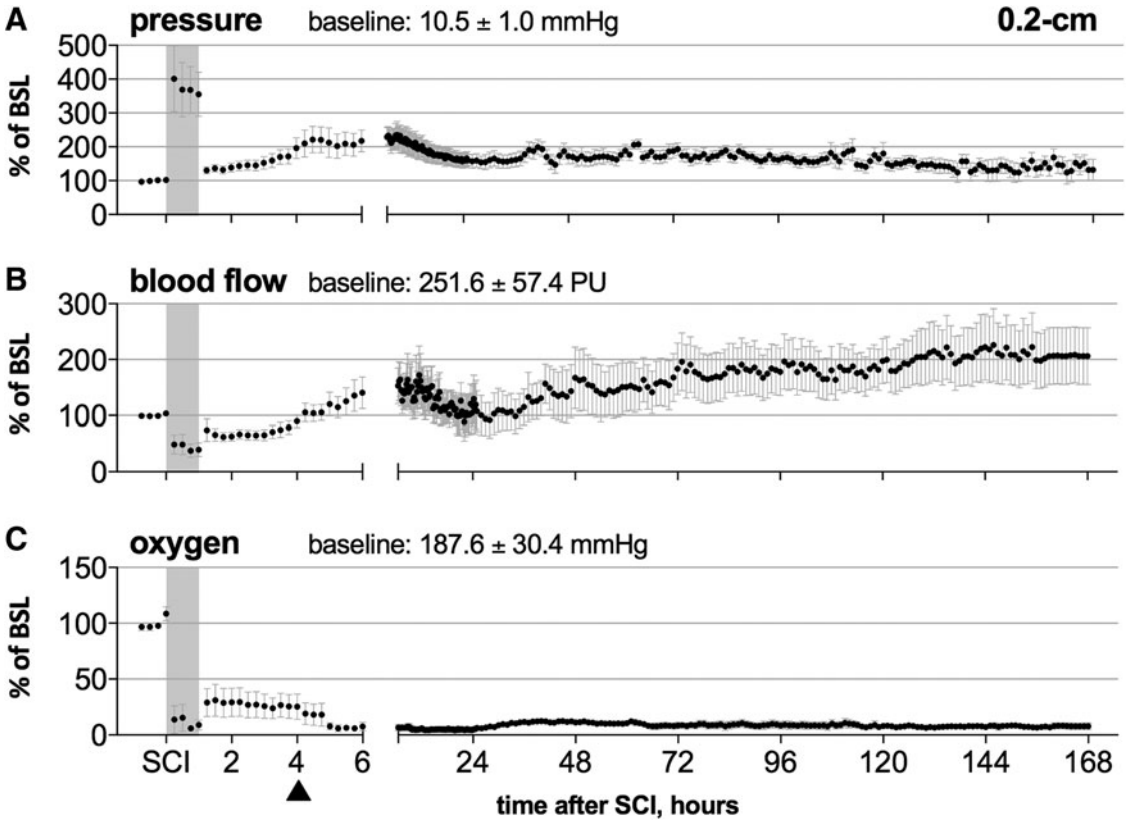

FIG. 5. Dynamic changes (%Δ) of blood flow, partial pressure of oxygen and pressure in the penumbra (0.2 cm) of the traumatic spinal cord injury site. The percentage change (%Δ) is calculated using an average of 60 min of baseline before SCI. **(A)** Intraparenchymal spinal cord pressure, **(B)** spinal cord blood flow (SCBF), **(C)** and partial pressure of oxygen ($PaPO_2$) responses before, during and after 1 h spinal cord contusion/compression (gray shading). SCI resulted in a prompt increase in cord pressure and a loss of SCBF with a critical reduction in $PaPO_2$. Following decompression, spinal cord pressure decreased sharply; however, it increased again within hours and remained consistently elevated for days. Within hours of decompression, SCBF restored to within baseline levels and continued to increase up to 200% above baseline levels by Day 7. Decompression only partially restored $PaPO_2$ and throughout the 7-day monitoring period seemed entirely unaffected. The dashed line at the 4 h post-SCI mark (▲) represents the discontinuation of anesthesia and ventilation at the end of the surgical procedure. BSL, baseline; SCI, spinal cord injury.

Downloaded by UNIVERSITE DE SHERBROOKE from www.liebertpub.com at 03/09/18. For personal use only.

~1400% that persisted for several days. Glycerol levels exhibited a peak value of 272% ± 48.2 within 30 min after contusion and remained around this level throughout the compression period (Fig. 7B). Immediately after decompression, levels increased again and remained high at around 325% for a period of 12 h. This was followed by a gradual decline to almost 60% of baseline values as of Day 2.

At the 0.2-cm position, glucose levels declined rapidly during the 60-min sustained compression period to a value as low as 60% of baseline (Fig. 8A). Decompression was not associated with an increase in glucose, and levels remained well below baseline (~65%) for up to 5 h after decompression. Subsequently, glucose levels returned nearly to baseline values within 24 h of SCI. Elevated lactate and decreasing pyruvate levels were observed during SCI (Fig. 8B, 8C), resulting in a marked rise in L/P ratio to above 700% within 60 min of sustained compression (Fig. 8D). After decompression, both lactate and pyruvate levels steadily increased up to 24 h after injury but proceeded to decrease after that point. As lactate levels did not change in direct proportion to pyruvate, the L/P ratio declined within the first 24 h followed by a gradual progressive rise until the end of the experiment (reaching nearly 350% at end of experiment). Throughout the entire post-injury period, the L/P ratio remained above baseline values.

At the 2.2-cm position, glutamate levels showed a similar pattern to the 0.2 cm probe, although far less pronounced (reaching close to 850%; Fig. 7A; open squares). After SCI, glycerol levels were elevated to about 225% from baseline but then declined, although they remained elevated above baseline for the first 4 h after injury (Fig. 7B).

A modest increase in glucose levels was observed acutely after SCI to around 140% at the 2.2-cm location, which quickly returned to baseline levels within minutes (Fig. 8A). Cessation of anesthesia and mechanical ventilation also coincided with a slight and transient increase above baseline. Lactate levels steadily increased to just above 150% during the first 24 h, followed by a decrease (Fig. 8B). Acutely after SCI, pyruvate levels also rose to about 150% before levels dropped to within or below baseline values (Fig. 8C). A steady rise in L/P ratio was detected after SCI, resulting in an increase in L/P ratio similar to the 0.2-cm probe, reaching a value of about 300% at Day 7 (Fig. 8D).

Relationships between tissue hemodynamics, hydrostatic pressure, and metabolic responses

Changes in SCBF, $PaPO_2$, and pressure during and after SCI were compared with changes in microdialysis data to define the

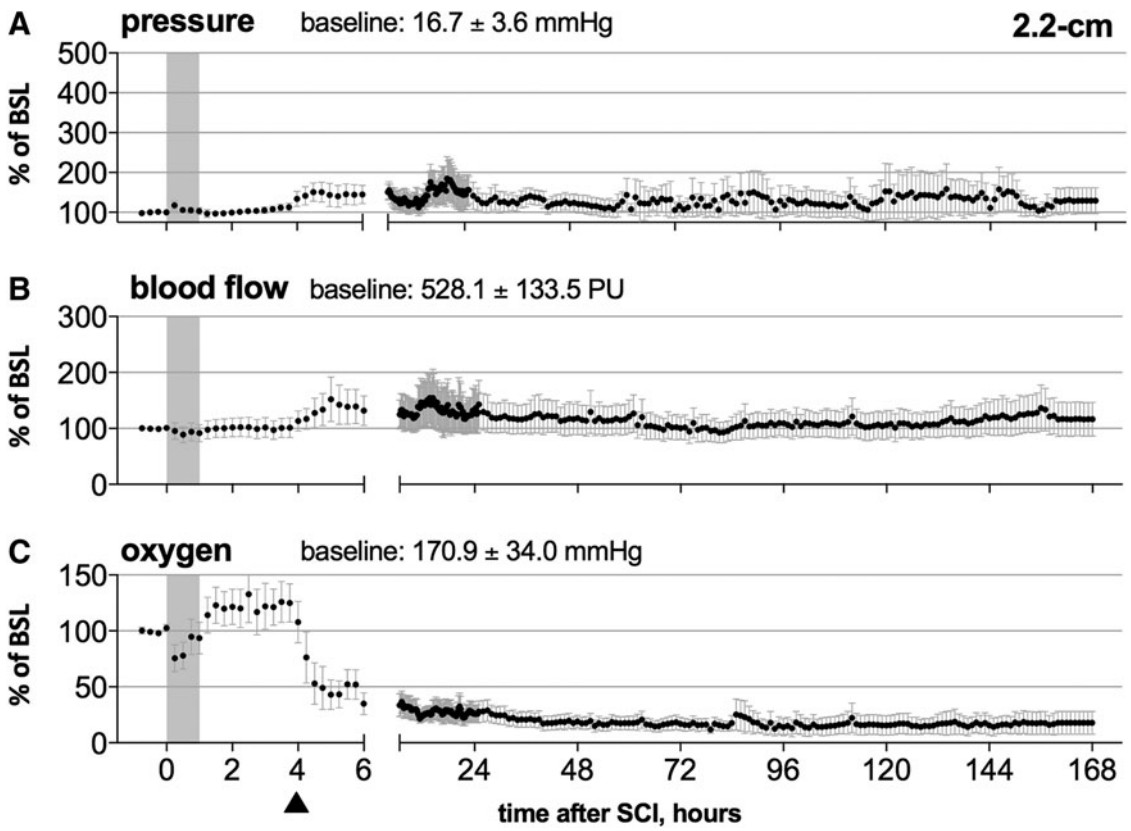

FIG. 6. Dynamic changes (%Δ) of blood flow, partial pressure of oxygen ($PaPO_2$), and pressure distal (2.2 cm) to the traumatic spinal cord injury site. The percentage change (%Δ) is calculated using an average of 60 min of baseline before SCI. **(A)** Intraparenchymal spinal cord pressure, **(B)** spinal cord blood flow (SCBF), and **(C)** $PaPO_2$ responses before, during and after 1 h spinal cord contusion/compression (gray shading). Following SCI a gradual increase in intraparenchymal pressure was observed during the first 24 h after which levels dropped back to baseline levels. SCBF seemed rather stable throughout the experiment. We observed a slow progressive decrease in $PaPO_2$ over time. The dashed line at the 4 h post-SCI mark (▲) represents the discontinuation of anesthesia and ventilation at the end of the surgical procedure. BSL, baseline; SCI, spinal cord injury.

Downloaded by UNIVERSITE DE SHERBROOKE from www.liebertpub.com at 03/09/18. For personal use only.

relationship between these parameters. Spearman correlation coefficients are presented in Supplementary Tables 1 and 2 (see online supplementary material at www.liebertpub.com). We divided the entire dataset into three different time-points after injury based on the metabolic response defined by the L/P ratio (marker of hypoxia) as follows: 0–1 h post-SCI (the first hour immediately following the initial impact, which includes compression of the spinal cord marked by a dramatic increase in L/P ratio); 2) 1–24 h post-SCI (the early 24 h ''acute'' phase after decompression/reperfusion, marked by a continual decrease in L/P ratio); and 3) 25–156 h after SCI (the ''sub-acute'' phase after decompression/reperfusion, marked by a secondary increase in L/P ratio). The Bonferroni correction for alpha with 36 comparisons is $p < 0.001$

Following SCI and during compression of the spinal cord, changes in SCBF at the 0.2-cm location positively correlated with changes in pyruvate ($r = 0.967$; $p < 0.001$), and $PaPO_2$ ($r = 0.967$; $p < 0.001$). Though not maintaining statistical significance after correction for multiple comparisons, there was a trend towards a positive relationship between SCBF and glucose ($r = 0.867$; $p = 0.005$) and a negative relationship between SCBF and the L/P ratio ($r = -0.833$; $p < 0.008$). Similarly, a strong negative correlation was observed between changes in glucose and an increase in L/P ratio ($r = -0.933$; $p < 0.001$). No significant relation was found between $PaPO_2$ and L/P ratio after correction for multiple comparisons ($r = -0.783$; $p = 0.017$). Notably, the magnitude of spinal cord pressure changes positively correlated with glutamate release ($r = 0.833$; $p = 0.008$).

Following the first 24 h after decompression, strong relationships between SCBF, glucose, and L/P ratio also were observed, akin to the early (0–1 h) SCI phase. SCBF positively correlated with change in glucose ($r = 0.785$; $p < 0.001$) and pyruvate levels ($r = 0.886$; $p < 0.001$), and negatively correlated with changes in L/P ratio ($r = -0.858$; $p < 0.001$) and glycerol levels ($r = -0.765$; $p < 0.001$). Glucose levels also correlated with increased pyruvate levels ($r = 0.765$; $p < 0.001$) levels and decreased L/P ratio ($r = -0.719$; $p < 0.001$). Additionally, changes in spinal cord pressure positively correlated with changes in SCBF ($r = 0.813$; $p < 0.001$).

During the later days after decompression (Days 1–7), a decrease in spinal cord pressure was associated with enhanced SCBF ($r = -0.551$; $p < 0.001$). Further, a negative correlation was found between $PaPO_2$ and L/P ratio ($r = -0.900$; $p < 0.001$). Contrary to the results of the prior two phases, SCBF correlated negatively with $PaPO_2$ ($r = -0.465$; $p < 0.001$) and positively with L/P ratio ($r = 0.845$; $p = 0.002$) during the late decompression phase. This apparent uncoupling of SCBF and $PaPO_2$ during this late phase was not observed at the 2.2-cm location.

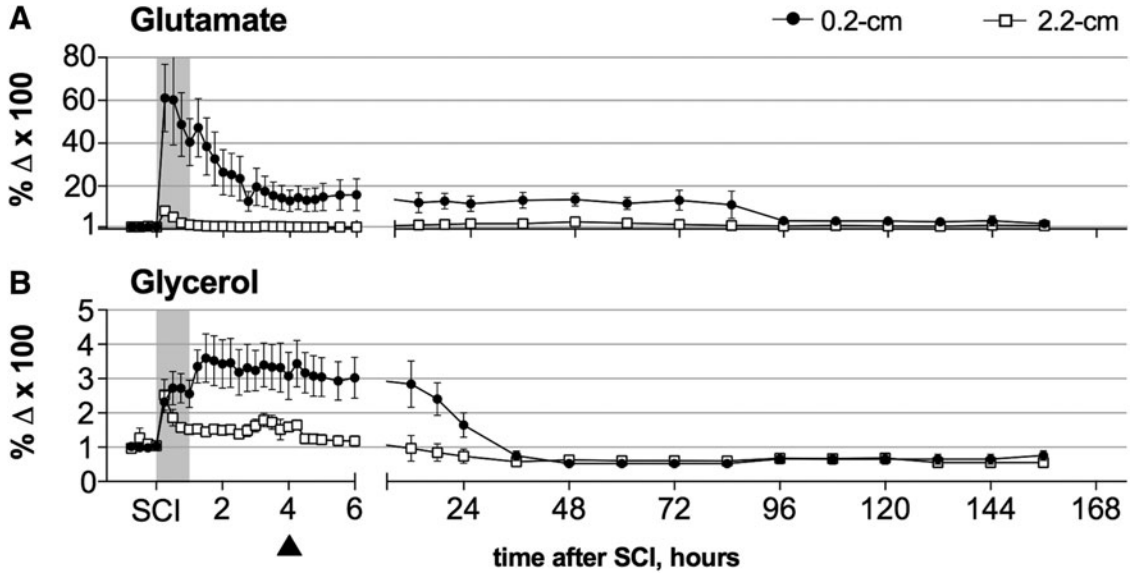

FIG. 7. Microdialysis measurements of intraparenchymal glutamate and glycerol changes (%Δ) in response to SCI at 0.2 and 2.2 cm from injury. The percentage change (%Δ) is calculated using the average of measurements obtained through 60 min of baseline recordings just prior to the SCI. **(A)** glutamate and **(B)** glycerol responses before, during and after 1 h spinal cord contusion/compression (gray shading). At the 0.2-cm position (•), an increase in glutamate and glycerol levels was observed upon SCI. The slope of glycerol increase was not as steep as that of glutamate and peaked later, but the increase was more sustained. Additionally, glycerol levels increased after decompression while glutamate levels remained unchanged. At the 2.2-cm position (□), a similar SCI-pattern for glutamate and glycerol was observed, although the responses were modest compared to the responses within the penumbra (0.2 cm). The dashed line at the 4 h post-SCI mark (▲) represents the discontinuation of anesthesia and ventilation at the end of the surgical procedure. SCI, spinal cord injury.

Downloaded by UNIVERSITE DE SHERBROOKE from www.liebertpub.com at 03/09/18. For personal use only.

Discussion

Pre-clinical studies by Tator and Fehings[2] and others[8–12] have revealed that vascular disruption and inadequate perfusion are key factors contributing to the development of secondary ischemic damage to the traumatically injured spinal cord. Intraparenchymal hemorrhage, vasospasm, impaired autoregulation, and vasogenic edema contribute to spinal ischemia, hypoxia, and energy dysfunction, of which all have a significant impact on tissue and functional recovery. Clinical treatment options to mitigate the effect of these responses are limited to early surgical decompression and aggressive hemodynamic support to improve spinal cord perfusion.[3,4] Given that aggressive hemodynamic support with the augmentation of MAP to 85–90 mm Hg may improve neurologic recovery in acute human SCI,[7] having an understanding of the post-traumatic alterations in SCBF and downstream consequences is central to the management of SCI patients.

Here, spatial and temporal dynamics of local SCBF, tissue oxygenation, pressure, and metabolism were investigated in the ''penumbra'' surrounding a traumatic SCI using a porcine model. This was achieved by simultaneously collecting data with laser Doppler/oxygen probes, pressure sensors, and microdialysis probes positioned in close proximity to one another within the spinal cord for 7 days post-injury. To our knowledge, this represents the first description of combined and continuous intraparenchymal physiologic and metabolic measures (perfusion, oxygenation, pressure, and microdialysis) over the first 7 days after traumatic spinal cord contusion/compression injury. We divided the entire dataset into three different time-points after injury: 1) 0–1 h post-SCI—the first hour immediately following the initial impact, which includes compression of the spinal cord; 2) 1–24 h post-SCI—the early 24 h ''acute'' phase after decompression/reperfusion; and 3) 25–156 h after SCI—the ''sub-acute'' phase after decompression/reperfusion.

First, during the initial 1 h of compression following contusive impact, tissue pressure markedly increased and was accompanied by a severe reduction in SCBF, low $PaPO_2$ levels, and a dramatic increase in L/P ratio, as well as in glutamate and glycerol levels. Second, during the first day (~24 h) following decompression, SCBF increased towards pre-injury baseline levels and then surpassed it. This is accompanied by a significant reduction in the L/P ratio, but only a limited and incomplete recovery of $PaPO_2$. Finally, between post-injury Days 1 and 7, SCBF increased to about 200% of baseline levels and underwent a transition from being positively correlated with $PaPO_2$ to being negatively correlated. During this late phase of apparent uncoupling of SCBF and $PaPO_2$, L/P ratio values increased consistently throughout the 7-day period. Further from the injury site (at the 2.2 cm probe position), the perturbations in SCBF, $PaPO_2$, and cord pressure were modest, with only a subtle increase in cord pressure over 7 days. This was nevertheless accompanied by a continuous increase in the L/P ratio. Various articles have demonstrated that probe insertion results in ''probe encapsulation'' and initiates an inflammatory response around the probe that can affect the recovery of small molecules, such as glucose.[24,25] These changes usually begin 24–36 h after probe implantation.[26] Because of the 7-day duration of our experiments, it is certainly possible that such probe encapsulation might occur. We acknowledge that this complicates the interpretation of our results, and hence the physiologic responses to traumatic SCI measured in the latter days of our study might be an underestimation of what is actually occurring.

While there are many published animal studies that have characterized the effect of traumatic injury on SCBF, most have utilized

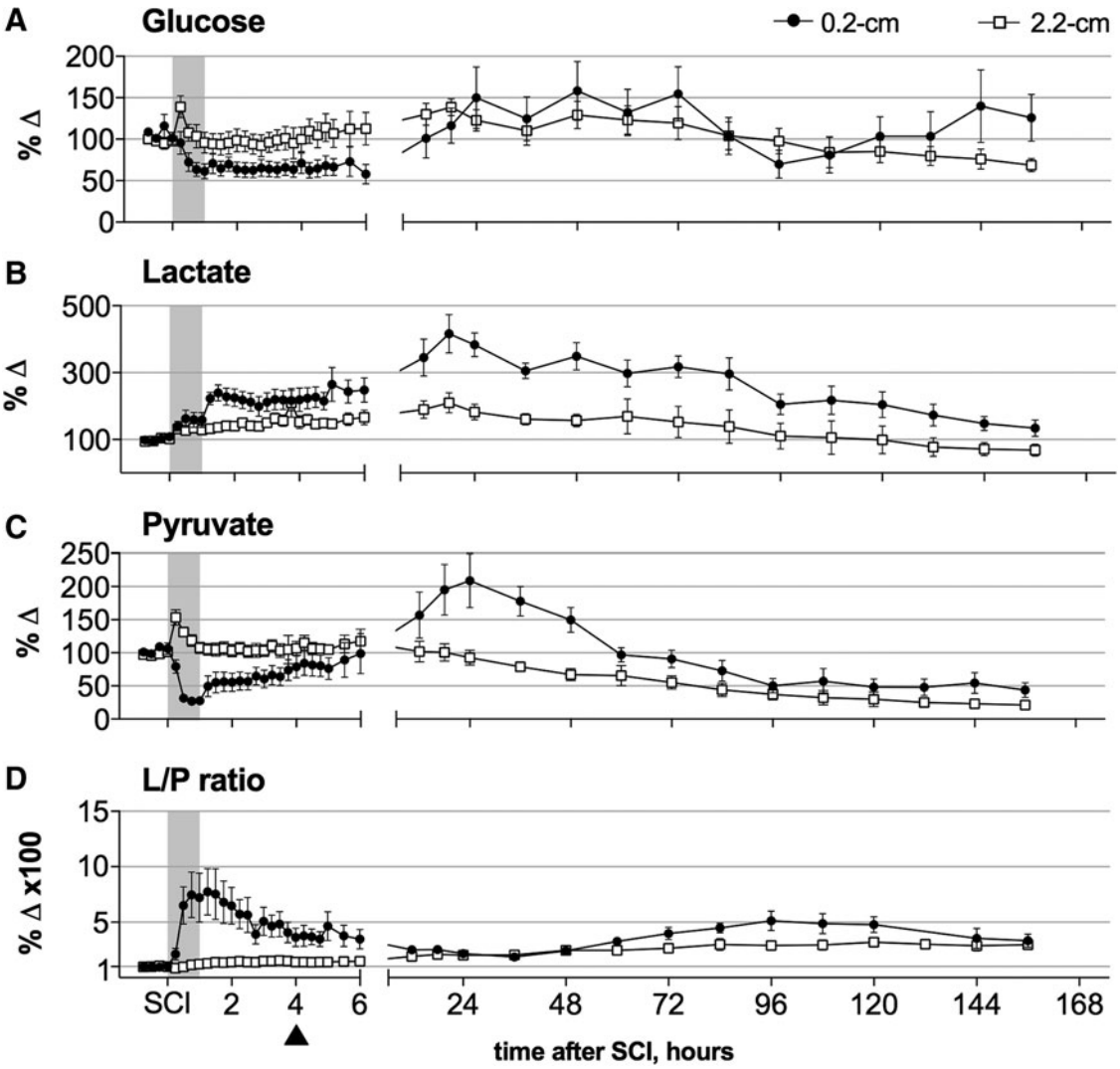

FIG. 8. Microdialysis measurements of intraparenchymal glucose, lactate, and pyruvate (%Δ) in response to SCI at 0.2 and 2.2 cm from injury. The percentage change (%Δ) is calculated using the average of measurements obtained through 60 min of baseline recordings just prior to the SCI. **(A)** Glucose, **(B)** lactate, **(C)** pyruvate, and **(D)** lactate to pyruvate (L/P) ratio responses before, during, and after 1 h spinal cord contusion/compression (gray shading). At the 0.2-cm position (●), glucose values decreased significantly upon SCI, and subsequently returned to baseline by Day 1. Within minutes after SCI, we observed an increase in lactate, a decrease in pyruvate, and a resulting increase in L/P ratio. After decompression, glucose, pyruvate and lactate increased while L/P ratio declined to 200% above baseline at 24 h. Thereafter, both lactate and pyruvate levels decreased again, although pyruvate fell proportionately more, resulting in a subsequent rise in L/P ratio till the end of the experiment (500% above baseline). At the 2.2-cm position (□), a slight increase in glucose levels was observed within the first 24 h after SCI; however, levels retuned to baseline thereafter. Within hours after SCI, we observed a slow but steady rise in lactate while pyruvate levels remained unchanged, producing an increase in L/P ratio. After 24 h, we observed a drop in lactate and a simultaneous and disproportionately greater drop in pyruvate, resulting in a continuous increase in L/P ratio to 500% above baseline at Day 7. The dashed line at the 4 h post-SCI mark (▲) represents the discontinuation of anesthesia and ventilation at the end of the surgical procedure. SCI, spinal cord injury.

rodent models with SCI induced by extradural clip compression for relatively short durations (1 min up to 40 min).[10–13] A few investigators have employed ongoing compression for 3 h up to 3 days using a metal rod placed on the dorsal dura of the spinal cord or by inserting a water-absorbing urethane polymer under the lamina.[27,28] Although different injury models and techniques of assessing blood flow were used (laser Doppler flowmetry, hydrogen clearance, microspheres) these compressive SCI models generally have reported acute decreases in SCBF in white and gray matter at and around the injury site, although Kobrine and colleagues have reported hyperemia during compression.[29] The latter is generally observed with lesser severities of injury. Further, it has been shown that functional recovery is dependent on the return of blood flow, which is in turn proportionate to the duration and severity of the compression.[30–32] In animal studies that have employed a contusive injury mechanism[9,33–39] the effect on SCBF is not as consistent. However, it is important to remember that traumatic human SCI is typically caused by a sudden, high-velocity contusive injury followed by periods of sustained compression (often for many hours to days). Besides our study, only a few other articles have evaluated SCBF in a combined contusion/compression model of SCI.[40,41] Kubota and colleagues[40] found a significant reduction in SCBF

Downloaded by UNIVERSITE DE SHERBROOKE from www.liebertpub.com at 03/09/18. For personal use only.

Downloaded by UNIVERSITE DE SHERBROOKE from www.liebertpub.com at 03/09/18. For personal use only.

during spinal cord compression following an initial contusion injury of the cord, which is consistent with our findings. Conversely, Sjovold[41] showed an elevated SCBF that steadily increased over 60 min of compression; however, Sjovold does state that the SCBF response varied considerably across individual animals. Nonetheless, while focusing on post-traumatic changes in SCBF can provide important insights, most studies only largely extend for the duration of the surgery and knowledge of the long-term monitoring of SCBF after SCI is limited.

Additionally, it is ultimately desirable to understand the subsequent downstream metabolic consequences of these changes within the areas of potentially vulnerable spinal cord tissue. As the balance between SCBF and metabolic rate of oxygen influences whether the tissue is hypoxic or not, monitoring SCBF alone may not provide a complete picture of the metabolic insult within the injury penumbra. For these reasons, we concurrently evaluated post-traumatic changes in SCBF and $PaPO_2$, as well as metabolic responses in a large animal model of contusion/compression SCI.

Adjacent to the impact site (represented by our 0.2 mm probe position), our data revealed a significant reduction in SCBF and $PaPO_2$ immediately following SCI while the cord remained compressed, reflecting severe compression-induced hypoperfusion. The rapid drop in glucose can be attributed to impaired blood flow as well as rapid conversion of local glucose into pyruvate, as supported by the close correlations between these parameters. In accordance with our previous study,[14] the increased lactate and decreased pyruvate resulting in an elevated L/P ratio is indicative of anaerobic glycolysis due to ischemia/hypoxia within the spinal cord. Glutamate increased immediately and remained elevated for days, indicating cellular release and/or lack of re-uptake, which is hampered by lack of adenosine triphosphate (ATP) and breakdown of membrane potentials in both neurons and glial cells. Cellular release of glutamate, as observed in several other studies, is mainly due to release of metabolic pools from neuronal and glial cell bodies, while the transmitter pool of glutamate contributes only a small fraction of early release.[42] In the present experiments, the increase of glycerol is likely a reflection of cellular membrane damage and breakdown of glycerol-containing phospholipids. A small fraction of glycerol also can be potentially generated as a byproduct of the glycolytic pathway in the post-traumatic scenario.[43–45] However, during profound ischemia, ATP deficiency would favor pyruvate and lactate instead of glycerol production. Further, glucose levels approached zero in microdialysate samples, which makes *de novo* synthesis of glycerol from glucose unlikely during this time period immediately after SCI while the cord remains compressed.

Immediately following the decompression, we observed SCBF and glucose to recover only partially ($\sim$25%), most likely due to the proximity to the injury and structural damage of microvasculature. $PaPO_2$ changed in proportion to blood flow, as one would expect if oxygen delivery were limited by SCBF. The drop in pyruvate observed during the immediate phase after SCI was gradually restored following partial return of blood flow and glucose. Accumulation of lactate with the L/P ratio remaining above baseline levels suggests ongoing anaerobic glycolysis in the ischemia/hypoxic lesion area. The strong negative correlation between $PaPO_2$ levels and the L/P ratio (i.e., low $PaPO_2$ is related to high L/P ratio) indicates that the persistent poor oxygenation might be the driving force for the continual increase in L/P ratio, as the increase in oxygen consumption exceeds oxygen availability.

For glycerol, there was a further increase at decompression followed by a reduction 1 day after the primary SCI, which may indicate reperfusion injury associated with reestablishing the blood supply. The interpretation of what is driving the glycerol levels is rather complicated by the existence of other sources of glycerol, transferred from the bloodstream into CSF and central nervous system compartments when the blood–brain and blood–spinal cord barriers are damaged. However, available data after brain injury (both traumatic and subarachnoid hemorrhage) suggest that this process might not make a significant contribution to interstitial glycerol concentrations.[44,46] We therefore believe that the rise in glycerol reflects actual structural damage of cell membranes, rather than extrinsic delivery through a disrupted blood–spinal cord barrier.

Contrary to the positive correlation between SCBF and $PaPO_2$ observed during the immediate phase after SCI, a modest but statistically significant negative correlation was seen in the late phase after SCI (1–7 days). SCBF levels started to rise above baseline values at 48 h after SCI and continued to increase until the end of the experiment at 7 days. Comparable changes in blood flow have been observed after traumatic brain injury (TBI), with most TBI patients showing reduced cerebral blood flow during the first 12 h after injury, followed by hyperperfusion (and in some patients vasospasms) before blood flow eventually normalizes.[47] The rise in SCBF during this time may be attributed to hypoxia, which is known to cause vasodilation either by direct (inadequate O_2 to sustain smooth muscle contraction) or indirect (production of vasodilator metabolites) actions on cerebral microvasculature. In our experiment, however, the rise in SCBF during days 1 through 7 post-injury did not confer a measurable improvement in $PaPO_2$. This observation is consistent with that of Gupta and colleagues,[48] who also reported the lack of a direct correlation between cerebral blood flow and oxygenation in TBI patients. This suggests that mechanisms other than a sheer reduction in blood perfusion are responsible for the tissue hypoxia in the latter stages after acute SCI. Importantly, our findings also highlight that the degree of hypoxia in the injured spinal cord may be underestimated if we rely solely on measures of blood perfusion in the post-injury period.

One explanation for the persistently low $PaPO_2$ during Days 1 through 7 is the imbalance between oxygen delivery and oxygen consumption. The later could be due to mitochondrial dysfunction and ineffective ATP production during oxidation, observed in ischemic brain tissue and in spinal cord after injury.[49,50] Delivery also may be compromised by impaired intraparenchymal oxygen diffusion, leading to decreased proportion of oxygen extracted from the blood during capillary passage through the spinal cord tissue (oxygen extraction fraction; OEF). Microvascular edema might cause increased barriers for oxygen diffusion with reduction of cellular oxygen delivery, despite the observation of blood flow remaining above what would be considered to be ''ischemic'' levels. Irregular microvascular collapse could result in significant increases in tissue path lengths for oxygen, with perivascular edema contributing to further increases in diffusion barriers for oxygen delivery. Recent work by Østergaard and colleagues[47] has proposed that changes in capillary flow patterns may have substantial influence on the relationship between CBF, tissue oxygen tension, and OEF after TBI. Their model predicts that severely disturbed capillary flow patterns could cause a parallel reduction in tissue oxygen tension and OEF even when gross perfusion is maintained.

To our knowledge, the first experimental SCI study to directly quantify spinal cord edema and intraparenchymal cord pressure after traumatic SCI was reported by Saadoun and colleagues in 2008.[51] Using a Millar pressure-monitoring microcatheter (SPR-1000) 2 days post-injury, they reported mean cord pressures around

Downloaded by UNIVERSITE DE SHERBROOKE from www.liebertpub.com at 03/09/18. For personal use only.

27 mm Hg in the wild-type mice, which were significantly higher than in sham-operated animals (with pressures less than 10 mm Hg). Subsequent clinical studies by this same group have reported similar pressure increases in traumatic human SCI, in which intraspinal pressure (ISP) has been measured with a Codman pressure monitoring catheter placed into the intrathecal space directly at the site of spinal cord injury. Werndle and colleagues first reported in a series of 18 patients an increase in ISP to a mean of approximately 20 mm Hg over the first 9 days post-injury.[52] Such intraspinal pressures were found to be decreased with expansion duraplasty in a prospective series of 10 patients treated with duraplasty and laminectomy versus 11 patients with laminectomy alone.[53] An interesting case report of one patient from this series revealed that the intraspinal pressure as measured by the intrathecal pressure probe placed at the site of injury were correlated very closely to measurements determined by a pressure probe placed directly into the spinal cord.[54] This suggests that as long as the cord swells to fill the intrathecal space and presses up against the dura, the subdural pressure recordings reflect the intraparenchymal recordings. More recently, the Papadopoulos group also has reported on the use of microdialysis catheters (CMA61; CMA Microdialysis AB, Solna, Sweden) inserted under the arachnoid on the spinal cord surface in SCI patients.[55,56] They also documented metabolic derangements such as elevated glutamate, glycerol, and lactate/pyruvate ratio, with the latter being elevated even a week post-injury.

Our findings in the large animal model of SCI followed over 7 days reveal many similarities with the novel findings of the Papadopoulos group in human SCI. In our large animal model, we, too, observed a considerable increase in intraparenchymal pressure near the site of injury, doubling to $\sim$20 mm Hg in the first 48 h. Our intraparenchymal microdialysis monitoring revealed similar derangements in the metabolic responses, with increased glycerol and glutamate early post-injury and an elevated L/P ratio that was sustained out to 7 days post-injury. As expected, the hemodynamic and metabolic abnormalities were most pronounced near the site of injury and less so 2 cm farther from the injury site. However, we noted that the L/P ratio in our animals did continue to rise over Days 2–7 even at the more distal measurement site, suggesting a rostrocaudal expansion of potential ischemia over the 7 days. Combined, our results reveal a translational relevance of our experimental animal paradigm in studying these important hemodynamic and metabolic responses to acute SCI. Additionally, they support the recent contention from Saadoun and Papadopoulos that local monitoring of the injured spinal cord can provide novel insights into the pathophysiology of acute SCI that can be acted upon by clinicians with standard hemodynamic management strategies.[57] We recognize that there are many aspects of the pathophysiology of secondary cord edema that we have not studied, including, for example, the role that prostaglandin E2 (PGE2) may play. Of interest, PGE2 is thought to be a principle mediator vascular permeability and promoting local blood flow associated with edema seen during acute inflammation.[58] Its release has been reported after SCI in both CSF and spinal cord tissue,[59,60] and pursuing such downstream mediators would be a logical goal of further studies using our model.

The experimental paradigm we employed is extremely complex and demanding, and discussion of the limitations is warranted. Our experiments utilized the pig as a large animal model of SCI. While many fundamental insights into the local hemodynamic responses to SCI have been derived from rodent models, we contend that the porcine model represents a reasonable alternative, particularly for these types of acute studies of hemodynamic physiology. Relevant to this line of inquiry, the spinal cord macro- and micro-vasculature of the pig shares many similarities to humans,[61–63] making it a routinely utilized animal species for the modeling of ischemic thoracic SCI in the context of thoraco-abdominal aortic aneurysm repair.[64,65] These vascular similarities also would make the pig a useful species to study acute physiological responses in traumatic thoracic SCI. Despite this, we understand that our experimental paradigm still has important differences with the human SCI condition. While we simulated the contusive nature of human SCI, the latter is often accompanied by compression that may be sustained for hours to days before being surgically relieved, if at all. This was recently illustrated in the landmark 313 patient Surgical Trial of Acute Spinal Cord Injury Study,[66] where the average time of ''early decompression'' was 14.2 ± 5.4 h and that of ''late decompression'' was 48.3 ± 29.3 h. Our experimental paradigm utilized 1 h of compression, far exceeding the 1 min of compression typically utilized in the rodent clip compression model. While it would be interesting to continue the experiment with persistent compression beyond 1 h, there are some physiologic limitations for the animal, which under the current protocol undergoes almost 12 h of anesthesia, with ongoing blood loss from the large posterior exposure and extensive laminectomy. We would acknowledge, however, that prolonging the duration of compression and severity of contusion would provide additional insights into the heterogeneity of human SCI.

As mentioned earlier, there are numerous ways by which investigators have measured SCBF in animal models of SCI. LDF has been shown to be a valid method for assessing microvascular blood flow in tissues such as the spinal cord[67] and has been employed in various pre-clinical studies to quantitatively measure hemodynamic responses by using small probes placed over the dura at the spinal segment of interest.[13,36,41,68–73] While LDF cannot provide the absolute blood flow rates as the hydrogen clearance or the microsphere technique, LDF has been shown to be highly correlated with both.[67,74,75] One of our main considerations in the use of LDF for SCBF monitoring in our experimental paradigm was that it could be used post-operatively to continuously monitor SCBF over several days without requiring an anesthetic and endotracheal intubation for precise hydrogen delivery, as is required for the hydrogen clearance technique. Since motion artifact has been a recognized problem with LDF,[76] considerable effort was extended to rigidly stabilize the spinal cord column and the LDF probes.

From a translational perspective, our observations point to the potential importance of being able to monitor local tissue hemodynamics in the acutely injured spinal cord, as emphasized by work of Papadopoulos and colleagues. While we have taken advantage of the ability in an animal model to invasively monitor the spinal cord to derive direct intra-parenchymal measures of blood flow, oxygenation, pressure, and metabolic responses, application in humans would require a less invasive approach. We are nonetheless intrigued by the observation in our model of persistent ischemia around the injury site even at 7 days post-injury, which is the time at which current clinical practice guidelines suggest to stop aggressive MAP augmentation in patients with acute SCI. We also find that the measurement of SCBF alone does not paint the complete picture of what is occurring at a metabolic level within the spinal cord. This advocates for the application of multi-modal monitoring of the spinal cord, as is done in TBI. Given that we currently have few treatment options for acute SCI patients, such measures to monitor local tissue hemodynamics within the injured spinal cord are justified to optimize our treatment protocols in the acute post-

injury phase—a period where growing evidence points to an opportunity to improve neurologic recovery in human SCI.

Acknowledgments

The authors gratefully acknowledge the funding support of the United States Department of Defense, Spinal Cord Injury Research Program and also the ICORD Spinal Cord Equipment Fund. Dr. Kwon holds the Canada Research Chair in Spinal Cord Injury. The authors also acknowledge the tremendous support, commitment, and expertise of many individuals at the University of British Columbia Center for Comparative Medicine (CCM). These include Dr. Ian Welch (Director), Gordon Gray (Facilities Manager), the clinical veterinarians Dr. Cathy Schuppli, Dr. Shelly McErlane, Dr. Laura Mobrey, Dr. Tamara Godbey, and Dr. Po-Yan Chen, and the amazing team of veterinarian technicians, including Micky Burgess, Kate Cooper, Shanna Dumontier, Kris Gillespie, Rhonda Hildebrandt, Mark Huang, Nicole Jackson, Tina Jorgensen, Stephanie Laprise, Ava McHugh, Kayla Reich, and Belinda To. Only through the skills and dedication of the entire CCM team is it possible to conduct these complex and demanding SCI experiments.

Author Disclosure Statement

No competing financial interests exist.

References

1. Mautes, A.E., Weinzierl, M.R., Donovan, F., and Noble, L.J. (2000). Vascular events after spinal cord injury: contribution to secondary pathogenesis. Phys. Ther. 80, 673–687.
2. Tator, C.H. and Fehlings, M.G. (1991). Review of the secondary injury theory of acute spinal cord trauma with emphasis on vascular mechanisms. J. Neurosurg. 75, 15–26.
3. Ryken, T.C., Hurlbert, R.J., Hadley, M.N., Aarabi, B., Dhall, S.S., Gelb, D.E., Rozzelle, C.J., Theodore, N., and Walters, B.C. (2013). The acute cardiopulmonary management of patients with cervical spinal cord injuries. Neurosurgery 72 Suppl 2, 84–92.
4. Furlan, J.C., Noonan, V., Cadotte, D.W., and Fehlings, M.G. (2011). Timing of decompressive surgery of spinal cord after traumatic spinal cord injury: an evidence-based examination of pre-clinical and clinical studies. J. Neurotrauma 28, 1371–1399.
5. Casha, S. and Christie, S. (2011). A systematic review of intensive cardiopulmonary management after spinal cord injury. J. Neurotrauma 28, 1479–1495.
6. Consortium for Spinal Cord Medicine. (2008). Early acute management in adults with spinal cord injury: a clinical practice guideline for health-care professionals. J. Spinal. Cord Med. 31, 403–479.
7. Hawryluk, G., Whetstone, W., Saigal, R., Ferguson, A., Talbott, J., Bresnahan, J., Dhall, S., Pan, J., Beattie, M., and Manley, G. (2015). Mean arterial blood pressure correlates with neurological recovery after human spinal cord injury: analysis of high frequency physiologic data. J. Neurotrauma 32, 1958–1967.
8. Sandler, A.N. and Tator, C.H. (1976). Review of the effect of spinal cord trauma on the vessels and blood flow in the spinal cord. J. Neurosurg. 45, 638–646.
9. Sandler, A.N. and Tator, C.H. (1976). Effect of acute spinal cord compression injury on regional spinal cord blood flow in primates. J. Neurosurg. 45, 660–676.
10. Kang, C.E., Clarkson, R., Tator, C.H., Yeung, I.W.T., and Shoichet, M.S. (2010). Spinal cord blood flow and blood vessel permeability measured by dynamic computed tomography imaging in rats after localized delivery of fibroblast growth factor. J. Neurotrauma 27, 2041–2053.
11. Rivlin, A.S. and Tator, C.H. (1978). Regional spinal cord blood flow in rats after severe cord trauma. J. Neurosurg. 49, 844–853.
12. Guha, A., Tator, C.H., and Rochon, J. (1989). Spinal cord blood flow and systemic blood pressure after experimental spinal cord injury in rats. Stroke 20, 372–377.
13. Hamamoto, Y., Ogata, T., Morino, T., Hino, M., and Yamamoto, H. (2007). Real-time direct measurement of spinal cord blood flow at the site of compression: relationship between blood flow recovery and motor deficiency in spinal cord injury. Spine (Phila. Pa. 1976) 32, 1955–1962.
14. Okon, E.B., Streijger, F., Lee, J.H.T., Anderson, L.M., Russell, A.K., and Kwon, B.K. (2013). Intraparenchymal microdialysis after acute spinal cord injury reveals differential metabolic responses to contusive versus compressive mechanisms of injury. J. Neurotrauma 30, 1564–1576.
15. Streijger, F., Lee, J.H.T., Manouchehri, N., Melnyk, A.D., Chak, J., Tigchelaar, S., So, K., Okon, E.B., Jiang, S., Kinsler, R., Barazanji, K., Cripton, P.A., and Kwon, B.K. (2016). Responses of the acutely injured spinal cord to vibration that simulates transport in helicopters or mine-resistant ambush-protected vehicles. J. Neurotrauma 33, 2217–2226.
16. Streijger, F., Lee, J.H.T., Chak, J., Dressler, D., Manouchehri, N., Okon, E.B., Anderson, L.M., Melnyk, A.D., Cripton, P.A., and Kwon, B.K. (2015). The effect of whole-body resonance vibration in a porcine model of spinal cord injury. J. Neurotrauma 32, 908–921.
17. Jones, C.F., Cripton, P.A., and Kwon, B.K. (2012). Gross morphological changes of the spinal cord immediately after surgical decompression in a large animal model of traumatic spinal cord injury. Spine (Phila. Pa. 1976) 37, E890–E899.
18. Chavko, M., Koller, W.A., Prusaczyk, W.K., and McCarron, R.M. (2007). Measurement of blast wave by a miniature fiber optic pressure transducer in the rat brain. J. Neurosci. Methods 159, 277–281.
19. Leonardi, A.D.C., Bir, C.A., Ritzel, D.V., and VandeVord, P.J. (2011). Intracranial pressure increases during exposure to a shock wave. J. Neurotrauma 28, 85–94.
20. Bauman, R.A., Ling, G., Tong, L., Januszkiewicz, A., Agoston, D., Delanerolle, N., Kim, Y., Ritzel, D., Bell, R., Ecklund, J., Armonda, R., Bandak, F., and Parks, S. (2009). An introductory characterization of a combat-casualty-care relevant swine model of closed head injury resulting from exposure to explosive blast. J. Neurotrauma 26, 841–860.
21. Dennison, C.R., Wild, P.M., Byrnes, P.W.G., Saari, A., Itshayek, E., Wilson, D.C., Zhu, Q.A., Dvorak, M.F.S., Cripton, P.A., and Wilson, D.R. (2008). Ex vivo measurement of lumbar intervertebral disc pressure using fibre-Bragg gratings. J. Biomech. 41, 221–225.
22. Soicher J. (2015). Evaluating the feasibility of quantifying spinal cord swelling as a function of pressure using fiber optic pressure sensors. Electronic Theses and Dissertations (ETDs) 2008+. University of British Columbia. Available at: https://open.library.ubc.ca/cIRcle/collections/24/items/1.0167187. Accessed August 10, 2017.
23. Streijger, F., Lee, J.H.T., Manouchehri, N., Okon, E.B., Tigchelaar, S., Anderson, L.M., Dekaban, G.A., Rudko, D.A., Menon, R.S., Iaci, J.F., Button, D.C., Vecchione, A.M., Konovalov, A., Sarmiere, P.D., Ung, C., Caggiano, A.O., and Kwon, B.K. (2016). The evaluation of magnesium chloride within a polyethylene glycol formulation in a porcine model of acute spinal cord injury. J. Neurotrauma 33, 2202–2216.
24. Wisniewski, N., Rajamand, N., Adamsson, U., Lins, P.E., Reichert, W.M., Klitzman, B., and Ungerstedt, U. (2002). Analyte flux through chronically implanted subcutaneous polyamide membranes differs in humans and rats. Am. J. Physiol. Endocrinol. Metab. 282, E1316–E1323.
25. Wisniewski, N., Klitzman, B., Miller, B., and Reichert, W.M. (2001). Decreased analyte transport through implanted membranes: differentiation of biofouling from tissue effects. J. Biomed. Mater. Res. 57, 513–521.
26. Cirrito, J.R., May, P.C., O'Dell, M.A., Taylor, J.W., Parsadanian, M., Cramer, J.W., Audia, J.E., Nissen, J.S., Bales, K.R., Paul, S.M., DeMattos, R.B., and Holtzman, D.M. (2003). In vivo assessment of brain interstitial fluid with microdialysis reveals plaque-associated changes in amyloid-beta metabolism and half-life. J. Neurosci. 23, 8844–8853.
27. Mautes, A.E., Schröck, H., Nacimiento, A.C., and Paschen, W. (2000). Regional spinal cord blood flow and energy metabolism in rats after laminectomy and acute compression injury. European. J. Trauma 26, 122–130.
28. Kurokawa, R., Murata, H., Ogino, M., Ueki, K., and Kim, P. (2011). Altered blood flow distribution in the rat spinal cord under chronic compression. Spine (Phila. Pa. 1976) 36, 1006–1009.

Downloaded by UNIVERSITE DE SHERBROOKE from www.liebertpub.com at 03/09/18. For personal use only.

Downloaded by UNIVERSITE DE SHERBROOKE from www.liebertpub.com at 03/09/18. For personal use only.

29. Kobrine, A.I., Evans, D.E., and Rizzoli, H. (1978). Correlation of spinal cord blood flow and function in experimental compression. Surg. Neurol. 10, 54–59.
30. Carlson, G.D., Gorden, C.D., Nakazowa, S., Wada, E., Warden, K., and LaManna, J.C. (2000). Perfusion-limited recovery of evoked potential function after spinal cord injury. Spine (Phila. Pa. 1976) 25, 1218–1226.
31. Carlson, G.D., Warden, K.E., Barbeau, J.M., Bahniuk, E., Kutina-Nelson, K.L., Biro, C.L., Bohlman, H.H., and LaManna, J.C. (1997). Viscoelastic relaxation and regional blood flow response to spinal cord compression and decompression. Spine (Phila. Pa. 1976) 22, 1285–1291.
32. Carlson, G.D., Minato, Y., Okada, A., Gorden, C.D., Warden, K.E., Barbeau, J.M., Biro, C.L., Bahnuik, E., Bohlman, H.H., and Lamanna, J.C. (1997). Early time-dependent decompression for spinal cord injury: vascular mechanisms of recovery. J. Neurotrauma 14, 951–962.
33. Chehrazi, B.B., Scremin, O., and Decima, E.E. (1989). Effect of regional spinal cord blood flow and central control in recovery from spinal cord injury. J. Neurosurg. 71, 747–753.
34. Wu, X.H., Yang, S.H., Duan, D.Y., Cheng, H.H., Bao, Y.T., and Zhang, Y. (2007). Anti-apoptotic effect of insulin in the control of cell death and neurologic deficit after acute spinal cord injury in rats. J. Neurotrauma 24, 1502–1512.
35. Soubeyrand, M., Laemmel, E., Dubory, A., Vicaut, E., Court, C., and Duranteau, J. (2012). Real-time and spatial quantification using contrast-enhanced ultrasonography of spinal cord perfusion during experimental spinal cord injury. Spine (Phila. Pa. 1976) 37, E1376–E1382.
36. Soubeyrand, M., Laemmel, E., Court, C., Dubory, A., Vicaut, E., and Duranteau, J. (2013). Rat model of spinal cord injury preserving dura mater integrity and allowing measurements of cerebrospinal fluid pressure and spinal cord blood flow. Eur. Spine. J. 22, 1810–1819.
37. Cawthon, D.F., Senter, H.J., and Stewart, W.B. (1980). Comparison of hydrogen clearance and 14C-antipyrine autoradiography in the measurement of spinal cord blood flow after severe impact injury. J. Neurosurg. 52, 801–807.
38. Yeo, J.D., Hales, J.R., Stabback, S., Bradley, S., Fawcett, A.A., and Kearns, R. (1984). Effects of a contusion injury on spinal cord blood flow in the sheep. Spine (Phila. Pa. 1976) 9, 676–680.
39. Huang, L., Lin, X., Tang, Y., Yang, R., Li, A.H., Ye, J.C., Chen, K., Wang, P., and Shen, H.Y. (2013). Quantitative assessment of spinal cord perfusion by using contrast-enhanced ultrasound in a porcine model with acute spinal cord contusion. Spinal Cord 51, 196–201.
40. Kubota, K., Saiwai, H., Kumamaru, H., Kobayakawa, K., Maeda, T., Matsumoto, Y., Harimaya, K., Iwamoto, Y., and Okada, S. (2012). Neurological recovery is impaired by concurrent but not by asymptomatic pre-existing spinal cord compression after traumatic spinal cord injury. Spine (Phila. Pa. 1976) 37, 1448–1455.
41. Sjovold, S.G. (2006). Spinal cord tissue changes due to residual compression in a novel rat contusion model. Electronic Theses and Dissertations (ETDs) 2008+. University of British Columbia. Available at: https://open.library.ubc.ca/cIRcle/collections/24/items/1.0080765. Accessed August 20, 2017.
42. Danbolt, N.C. (2001). Glutamate uptake. Prog. Neurobiol. 65, 1–105.
43. Merenda, A., Gugliotta, M., Holloway, R., Levasseur, J.E., Alessandri, B., Sun, D., and Bullock, M.R. (2008). Validation of brain extracellular glycerol as an indicator of cellular membrane damage due to free radical activity after traumatic brain injury. J. Neurotrauma 25, 527–537.
44. Marklund, N., Salci, K., Lewén, A., and Hillered, L. (1997). Glycerol as a marker for post-traumatic membrane phospholipid degradation in rat brain. Neuroreport 8, 1457–1461.
45. Clausen, F., Hillered, L., and Gustafsson, J. (2011). Cerebral glucose metabolism after traumatic brain injury in the rat studied by 13C-glucose and microdialysis. Acta Neurochir. (Wien) 153, 653–658.
46. Hillered, L., Valtysson, J., Enblad, P., and Persson, L. (1998). Interstitial glycerol as a marker for membrane phospholipid degradation in the acutely injured human brain. J. Neurol. Neurosurg. Psychiatry 64, 486–491.
47. Østergaard, L., Engedal, T.S., Aamand, R., Mikkelsen, R., Iversen, N.K., Anzabi, M., Næss-Schmidt, E.T., Drasbek, K.R., Bay, V., Blicher, J.U., Tietze, A., Mikkelsen, I.K., Hansen, B., Jespersen, S.N., Juul, N., Sørensen, J.C.H., and Rasmussen, M. (2014). Capillary transit time heterogeneity and flow-metabolism coupling after traumatic brain injury. J. Cereb. Blood. Flow Metab. 34, 1585–1598.
48. Gupta, A.K., Hutchinson, P.J., Fryer, T., Al-Rawi, P.G., Parry, D.A., Minhas, P.S., Kett-White, R., Kirkpatrick, P.J., Mathews, J.C., Downey, S., Aigbirhio, F., Clark, J., Pickard, J.D., and Menon, D.K. (2002). Measurement of brain tissue oxygenation performed using positron emission tomography scanning to validate a novel monitoring method. J. Neurosurg. 96, 263–268.
49. Jia, Z.Q., Li, G., Zhang, Z.Y., Li, H.T., Wang, J.Q., Fan, Z.K., and Lv, G. (2016). Time representation of mitochondrial morphology and function after acute spinal cord injury. Neural. Regen. Res. 11, 137–143.
50. McEwen, M.L., Sullivan, P.G., Rabchevsky, A.G., and Springer, J.E. (2011). Targeting mitochondrial function for the treatment of acute spinal cord injury. Neurotherapeutics 8, 168–179.
51. Saadoun, S., Bell, B.A., Verkman, A.S., and Papadopoulos, M.C. (2008). Greatly improved neurological outcome after spinal cord compression injury in AQP4-deficient mice. Brain 131, 1087–1098.
52. Werndle, M.C., Saadoun, S., Phang, I., Czosnyka, M., Varsos, G.V., Czosnyka, Z.H., Smielewski, P., Jamous, A., Bell, B.A., Zoumprouli, A., and Papadopoulos, M.C. (2014). Monitoring of spinal cord perfusion pressure in acute spinal cord injury: initial findings of the injured spinal cord pressure evaluation study*. Crit. Care Med. 42, 646–655.
53. Phang, I., Werndle, M.C., Saadoun, S., Varsos, G., Czosnyka, M., Zoumprouli, A., and Papadopoulos, M.C. (2015). Expansion duroplasty improves intraspinal pressure, spinal cord perfusion pressure, and vascular pressure reactivity index in patients with traumatic spinal cord injury: injured spinal cord pressure evaluation study. J. Neurotrauma 32, 865–874.
54. Phang, I. and Papadopoulos, M.C. (2015). Intraspinal pressure monitoring in a patient with spinal cord injury reveals different intradural compartments: Injured Spinal Cord Pressure Evaluation (ISCoPE) Study. Neurocrit. Care 23, 414–418.
55. Phang, I., Zoumprouli, A., Papadopoulos, M.C., and Saadoun, S. (2016). Microdialysis to optimize cord perfusion and drug delivery in spinal cord injury. Ann. Neurol. 80, 522–531.
56. Chen, S., Phang, I., Zoumprouli, A., Papadopoulos, M.C., and Saadoun, S. (2016). Metabolic profile of injured human spinal cord determined using surface microdialysis. J. Neurochem. 139, 700–705.
57. Saadoun, S. and Papadopoulos, M.C. (2016). Spinal cord injury: is monitoring from the injury site the future? Crit. Care 20, 308.
58. Davies, P., Bailey, P.J., Goldenberg, M.M., and Ford-Hutchinson, A.W. (1984). The role of arachidonic acid oxygenation products in pain and inflammation. Annu. Rev. Immunol. 2, 335–357.
59. Marsala, M., Malmberg, A.B., and Yaksh, T.L. (1995). The spinal loop dialysis catheter: characterization of use in the unanesthetized rat. J. Neurosci. Methods 62, 43–53.
60. Bernards, C.M. and Akers, T. (2006). Effect of postinjury intravenous or intrathecal methylprednisolone on spinal cord excitatory amino-acid release, nitric oxide generation, PGE2 synthesis, and myeloperoxidase content in a pig model of acute spinal cord injury. Spinal Cord 44, 594–604.
61. Strauch, J.T., Lauten, A., Zhang, N., Wahlers, T., and Griepp, R.B. (2007). Anatomy of spinal cord blood supply in the pig. Ann. Thorac. Surg. 83, 2130–2134.
62. Etz, C.D., Kari, F.A., Mueller, C.S., Silovitz, D., Brenner, R.M., Lin, H.M., and Griepp, R.B. (2011). The collateral network concept: a reassessment of the anatomy of spinal cord perfusion. J. Thorac. Cardiovasc. Surg. 141, 1020–1028.
63. Christiansson, L., Ulus, A.T., Hellberg, A., Bergqvist, D., Wiklund, L., and Karacagil, S. (2001). Aspects of the spinal cord circulation as assessed by intrathecal oxygen tension monitoring during various arterial interruptions in the pig. J. Thorac. Cardiovasc. Surg. 121, 762–772.
64. Geisbüsch, S., Stefanovic, A., Koruth, J.S., Lin, H.M., Morgello, S., Weisz, D.J., Griepp, R.B., and Di Luozzo, G. (2014). Endovascular coil embolization of segmental arteries prevents paraplegia after subsequent thoracoabdominal aneurysm repair: an experimental model. J. Thorac. Cardiovasc. Surg. 147, 220–226.
65. Saether, O.D., Bäckström, T., Aadahl, P., Myhre, H.O., Norgren, L., and Ungerstedt, U. (2000). Microdialysis of the spinal cord during thoracic aortic cross-clamping in a porcine model. Spinal Cord 38, 153–157.
66. Fehlings, M.G., Vaccaro, A., Wilson, J.R., Singh, A., W Cadotte, D., Harrop, J.S., Aarabi, B., Shaffrey, C., Dvorak, M., Fisher, C., Arnold, P., Massicotte, E.M., Lewis, S., and Rampersaud, R. (2012). Early

versus delayed decompression for traumatic cervical spinal cord injury: results of the Surgical Timing in Acute Spinal Cord Injury Study (STASCIS). PLoS One 7, e32037.
67. Lindsberg, P.J., O'Neill, J.T., Paakkari, I.A., Hallenbeck, J.M., and Feuerstein, G. (1989). Validation of laser-Doppler flowmetry in measurement of spinal cord blood flow. Am. J. Physiol. 257, H674–H680.
68. Phillips, J.P., Cibert-Goton, V., Langford, R.M., and Shortland, P.J. (2013). Perfusion assessment in rat spinal cord tissue using photoplethysmography and laser Doppler flux measurements. J. Biomed. Opt. 18, 037005.
69. Lindsberg, P.J., Jacobs, T.P., Frerichs, K.U., Hallenbeck, J.M., and Feuerstein, G.Z. (1992). Laser-Doppler flowmetry in monitoring regulation of rapid microcirculatory changes in spinal cord. Am. J. Physiol. 263, H285–H292.
70. Yamada, T., Morimoto, T., Nakase, H., Hirabayashi, H., Hiramatsu, K., and Sakaki, T. (1998). Spinal cord blood flow and pathophysiological changes after transient spinal cord ischemia in cats. Neurosurgery 42, 626–634.
71. Westergren, H., Farooque, M., Olsson, Y., and Holtz, A. (2001). Spinal cord blood flow changes following systemic hypothermia and spinal cord compression injury: an experimental study in the rat using Laser-Doppler flowmetry. Spinal Cord 39, 74–84.
72. Martirosyan, N.L., Kalani, M.Y.S., Bichard, W.D., Baaj, A.A., Gonzalez, L.F., Preul, M.C., and Theodore, N. (2015). Cerebrospinal fluid drainage and induced hypertension improve spinal cord perfusion after acute spinal cord injury in pigs. Neurosurgery 76, 461–468.
73. Marsala, M., Sorkin, L.S. and Yaksh, T.L. (1994). Transient spinal ischemia in rat: characterization of spinal cord blood flow, extracellular amino acid release, and concurrent histopathological damage. J. Cereb. Blood Flow Metab. 14, 604–614.
74. Kramer, M.S., Vinall, P.E., Katolik, L.I., and Simeone, F.A. (1996). Comparison of cerebral blood flow measured by laser-Doppler flowmetry and hydrogen clearance in cats after cerebral insult and hypervolemic hemodilution. Neurosurgery 38, 355–361.
75. Skarphedinsson, J.O., Hårding, H., and Thorén, P. (1988). Repeated measurements of cerebral blood flow in rats. Comparisons between the hydrogen clearance method and laser Doppler flowmetry. Acta. Physiol. Scand. 134, 133–142.
76. Oberg, P.A. (1999). Tissue motion—a disturbance in the laser-Doppler blood flow signal? Technol. Health Care 7, 185–192.

Address correspondence to:
Brian K. Kwon, MD, PhD, FRCSC
Department of Orthopedics
University of British Columbia
6th Floor, Blusson Spinal Cord Center
Vancouver General Hospital
818 West 10th Avenue
Vancouver, British Columbia, Canada V5Z 1M9

E-mail: brian.kwon@ubc.ca

Downloaded by UNIVERSITE DE SHERBROOKE from www.liebertpub.com at 03/09/18. For personal use only.